

國立交通大學

材料科學與工程學系

博士論文

新穎碳基奈米材料在場發射應用上的合成與改質

Fabrication and Modification of New Carbon
Based Nanomaterials for Field Emission Devices



研究生：蔡佳倫

指導教授：陳家富博士

中華民國九十三年六月

新穎碳基奈米材料在場發射應用上的合成與改質
Fabrication and Modification of New Carbon Based
Nanomaterials for Field Emission Devices

研究生：蔡佳倫

Student : Chia-Lun Tsai

指導教授：陳家富

Advisor : Chia-Fu Chen

國立交通大學

材料科學與工程學系



Submitted to Department of Material Science and Engineering

College of Engineering

National Chiao Tung University

in partial Fulfillment of the Requirements

for the Degree of

Doctor of Philosophy

in

Material Science and Engineering

June 2004

Hsinchu, Taiwan

中華民國九十三年六月

新穎碳基奈米材料在場發射應用上的合成與改質

研究生：蔡佳倫

指導教授：陳家富 博士

國立交通大學材料與工程學系

摘 要

場發射顯示器是一個由許多場發射源組成的高亮度平面顯示器。在未來的平面顯示器中，場發射顯示器是一個令人值得期待的一個技術。由於深具潛力，奈米碳基材料已被視為場發射源的最佳材料之一。因此本論文的研究主要著重在如何提升奈米碳基材料的場發射電子特性。研究方向分為兩大類：第一則是材料改質，藉此提升材料場發射之電子特性。第二則是合成新穎的奈米碳基材料，利用其獨特的奈米效應來增加場發射電流。

在材料改質方面，主要是利用偏壓效應、P 型或 N 型之摻雜源與類鑽碳披覆來提升傳統碳基材料的電子特性。實驗結果顯示，偏壓效應除了可提升材料的成長速度，並可提供電場使材料在垂直基板方向成長。而在摻雜 N 型或 P 型的方面，提供多餘的電子或電洞明顯使單位面積的場發射電流密度增加。

而在合成新穎奈米碳基材料上，除了利用上述方法提升奈米碳管的場發射特性之外。我們也首先發表了新穎的奈米碳基材料：奈米石墨尖錐與奈米碳化鉻顆粒。相對於奈米碳管的石墨空心結構，穿透式電子顯微鏡發現奈米石墨尖錐呈現出石墨組成的實心結構與垂直基板的成長方向。此外，頂部的針狀結構亦提高了電子激發效率與場發射特徵常數(β)。若先鍍上一層鉻的金屬薄膜，可發現金屬鉻會被成長中的每根奈米石墨尖錐由下往上舉起，並逐漸碳化成一顆一顆的奈米碳化鉻顆粒。而這些奈米級大小的碳化鉻在場發射量測中，藉其本身的量子尺寸效應提供了較佳的表面電子傳輸，明顯地增加了場發射電流。這種自發性對位形成的微小奈米顆粒將可以被應用在許多方面。此外，利用半導體技術我們成功製造了一具有低孔徑 (4 微米) 的金屬/絕緣體/半導體 (MIS) 的三極場發射元件。元件中的閘極結構可輕易的激發電子跳出，除了增加場發射電流之外，也有效地降低起始電壓。

Fabrication and Modification of New Carbon Based Nanomaterials for Field Emission Devices

Student: Chia-Lun Tsai

Advisor: Dr. Chia-Fu Chen

Institute of Materials Science and Engineering

National Chiao Tung University

Abstract

Field emission display (FED) is a promising flat panel display in which the images are formed from large array of pixels, each addressed by controllable field emission sources. Recently, carbon based nanomaterials have attracted great interest owing to their potential application of field emission. This dissertation mainly aims at the improvement of carbon based nanomaterials on field emission characteristic. Research can be divided into two following categories. First is modifying materials' property in order to enhance their field emission characteristic. Second is fabricating new carbon based nanomaterials to increase their field emission currents by using their unique properties.

The bias effect; N or P-type dopants and diamond-like carbon cladding are used to improve field emission characteristics of materials. Experimental results indicate that bias effect would not only increase the growth rate but also lead to the well-aligned inclination. Doping additional electrons or holes into carbon material system results in the increase of field emission currents.

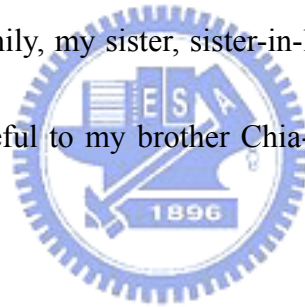
In the fabrication of new material field, graphite nanotip and itself capped with Cr nano particles have been first reported in the world. Compared to the hollow structure of nanotubes, graphite nanotips display the solid body and well aligned growth direction. The needle-like shape causes the electrons easily induced and larger field enhancement (β). Pre-deposition of Cr thin film will form the nanocrystalline chromium carbides on the top of the individual graphite nanotips, providing higher surface conductivity for electrons transportation. This self-alignment could be used in many applications. Moreover, low threshold voltage and high current density characterization is successfully achieved by using gated structure device.

Acknowledgment

Many people have assisted me during this dissertation work. I'm very grateful to my graduate advisor Prof. C. F. Chen, whose inspiration and guidance benefited me significantly; without his support, this work could not have been finished.

The author would like to acknowledge the financial support from the National Science Council of Taiwan. Thanks to Miss Jeng Mei-Li for providing access to the TEM. I would like to express my appreciation to my colleagues, especially the kindly discussion from Dr. Chien- Liang Lin.

Many thanks to my family, my sister, sister-in-law; and my lovely nephew and niece. I feel particularly grateful to my brother Chia-Fong Tsai, who helped me and cared me greatly in my life.



I really want to devote this dissertation to my parents, their endless love and spirit encouragement is my main motive power on research.

TABLE OF CONTENTS

	Page
ABSTRACT (CHINESE)	i
ABSTRACT (ENGLISH)	ii
ACKNOWLEDGEMENT	iii
TABLE OF CONTENTS	iv
LIST OF TABLES	viii
LIST OF FIGURES	ix
CHAPTER 1. INTRODUCTION	1
1.1 Preface	1
1.2 Why carbon-based materials?.....	2
1.3 Why nanosize requirement?.....	15
1.4 Advantage of field emission display.....	15
1.5 Motivation	19
1.6 Reference	21
CHAPTER 2. FUNDAMENTAL THEORY	24
2.1 Field Emission from metals	24
2.1.1 Field emission from semiconductor	26
2.1.2 Fowler-Nordheim equation for gated FEA	28
2.2 Bias enhances nucleation of diamond in microwave CVD	30
2.3 Reference	33
CHAPTER 3. EXPERIMENT METHOD	35
3.1 Experimental details.....	35
3.2 Bias assisted microwave plasma chemical vapor deposition system	35
3.3 Deposition conditions of various carbon-based nanomaterials...38	
3.4 Characterization of carbon-based nanomaterials.....	38
3.4.1 Scanning electron microscopy (SEM).....	38
3.4.2 Micro-Raman spectroscopy	38
3.4.3 Secondary ion mass spectrometry (SIMS)	41

3.4.4	Measurement of field emission characterization	41
3.4.5	Transmission electron microscopy (TEM)	42
3.4.6	Electron energy loss spectroscopy(EELS).....	42
3.5	Reference	46

CHAPTER 4. MODIFICATION OF SILICON NANO EMITTERS BY DIAMOND-CLAD PROCESS		47
4.1	Introduction	47
4.2	Experiment	48
4.3	Results and discussion	49
4.4	Conclusion	60
4.5	Reference	61

CHAPTER 5. CHARACTERIZATION OF NANOSIZED DIAMOND-LIKE CARBON EMITTERS ARRAYS		63
5.1	Introduction	63
5.2	Experiment.....	66
5.2.1	Deposition of silicon oxide by furnace and LPCVD system	66
5.2.2	Lithography	66
5.2.3	Deposition of Ti and Pt films as gated layer using dual-gun evaporator	66
5.2.4	Remove photoresist by lift-off process.....	67
5.2.5	Removal of silicon oxide layer by metal etcher system	67
5.2.6	Diamond-like carbon emitters deposition condition	
5.3	Results and discussion.....	70
5.4	Conclusion.....	85
5.5	Reference.....	86

CHAPTER 6. BIAS AND REACTIVE GASES EFFECTS ON THE GROWTH OF CARBON NANOTUBES		89
6.1	Introduction	89
Part A	Bias effect on the growth of carbon nanotubes.....	90
6.2A	Experiment.....	90
6.3A	Results and discussion.....	90

Part B	Reactive gas effect on the growth of carbon nanotubes.....	104
6.2B	Experiment.....	104
6.3B	Results and discussion.....	104
6.4	Conclusion.....	118
6.5	Reference.....	119

CHAPTER 7. CHARACTERIZATION OF BORON-DOPED CARBON

	NANOTUBE ARRAYS.....	121
7.1	Introduction.....	121
7.2	Experiment.....	121
7.3	Results and discussion.....	123
7.4	Conclusion.....	143
7.5	Reference.....	145

CHAPTER 8. FIELD EMISSION FROM WELL-ALIGNED CARBON

	NANOTIPS.....	147
8.1	Introduction.....	147
Part A	Field emission of well-aligned carbon nanotips in diode structure.	
	148
8.2A	Experiment.....	148
8.3A	Results and discussion.....	148
Part B	Field emission of well-aligned carbon nanotips in gated structure.	
	158
8.2B	Experiment.....	158
8.3B	Results and discussion.....	158
8.4	Conclusion.....	166
8.5	Reference.....	167

CHAPTER 9. SELF-EMBEDDED OF NANOCRYSTALLINE CHROMIUM

	CARBIDES ON WELL-ALIGNED CARBON NANOTIPS	169
9.1	Introduction.....	169
9.2	Experiment.....	170
9.3	Results and discussion.....	171
9.4	Conclusion.....	182

9.5	Reference	183
	CHAPTER 10. CONCLUSION	184
	LIST OF PUBLICATIONS	187
	RESUME	190



LIST OF TABLES

	Page
5.1 Conditions of deposited Ti and Pt layers	67
5.2 Deposition conditions of undoped, boron and phosphours-doped DLC emitters, respectively	69
6.1 Summaries of the comparison of CNTs grown with CH ₄ /H ₂ and CH ₄ /CO ₂ mixtures.....	113
6.2 Deposition conditions of low temperature growth of carbon nanofibers	115
7.1 Deposition conditions undoped and boron-doped carbon nanotubes	122
8.1 Deposition conditions of carbon nanotips.....	158



LIST OF FIGURES

		Page
1.1	(a) orientational correlations and intermolecular interactions of C ₆₀ and C ₇₀ . (b) spherical-like carbon onions [9].....	7
1.2	(a) TEM images as the indicated magnification of Ni catalyzed nanofibers [10]; (b) SEM image of as-grown MWNT and (c) HRTEM image of individual MWNT. Inset-figure shows the (002) diffraction spots [11]	8
1.3	Optimized structures for a T carbon nanotube junction obtained using a GTBMD simulation [22]	9
1.4	(a) CNTs grown on Si substrate, there are Y and H-junction CNTs and 3D CNT webs. (b) H-junction or multiple Y-junction CNTs on the substrate [23].....	10
1.5	(a) TEM images of hollow rectangular parallelepiped graphitic cages and (b) breakage of graphitic layers can be seen at corners A-D [24]	11
1.6	(a) SEM image of SWNT rings and (b) TEM image of a section of the ring and (c) Histogram showing distribution of ring radii [25]	12
1.7	(a) TEM images (with scale bar=200 nm) of the carbon nanocones and (b) Five different types of cones in a-e (with scale bar = 200 nm). Magnified image of a cone tip is shown in f (with scale bar=5 nm) [26]	13
1.8	(a) TEM images of uniformly shaped spherical particles (b) image of a particle, showing aggregation of tube-like structures; and (c) Conical horn-like tips can be seen at the end of the tube-like structure [27]	14
1.9	Schematic cross section of a Field Emission Display.....	18
2.1	Diagram of potential energy of electrons at the surface of metal	24
2.2	Diagram of potential energy of electrons at the surface of an n-type semiconductor with field penetration into semiconductor interior	27
2.3	Schematic diagram of a cell of a microfabricated gated FEA	28
3.1	Schematic diagram of the bias assisted microwave plasma CVD system.....	37
3.2	Raman spectrum of the CVD diamond film grown on a Fused quartz substrate. Insert: optical micrograph displaying the morphology	40
3.3	The scheme of the instrument of the I-V measurement	44
3.4	(a) EELS spectra of graphite, diamond, amorphous (hydrogenated) carbon, in the 280-296 eV region; (b) the EELS spectrum for an ion-grown carbon filament in the 0-40 eV range	45
4.1	(a) High and (b) low magnification of SEM photographs of Si nanotips.....	50

4.2	TEM of (a) Si tips and (b) high-resolution images of individual Si tip.....	51
4.3	(a) High and (b) low magnification of SEM photographs of DLC-clad Si nanotips.....	52
4.4	AES profile of DLC-clad Si tips.....	54
4.5	AES surface survey of DLC-clad Si tips.....	55
4.6	Raman spectrum of DLC-clad Si nanotips.....	57
4.7	Electric field (E) versus current density (J) of Si and DLC-clad Si tips, respectively.....	60
5.1	Fabricated procedure of diamond-like carbon emitters on the FEAS with gated diode pattern.....	65
5.2	SEM photographs of MIS diode structure with 50 x 50 circles.....	68
5.3	SEM photographs of undoped diamond-like carbon emitters -grown under condition C.....	71
5.4	SEM photographs of undoped diamond-like carbon emitters with various methane concentrations (a) sample A, (b) sample B and (c) sample C, respectively.....	72
5.5	The SEM photograph of phosphorus-doped diamond-like carbon emitters with various doping concentration (a) 2sccm, (b) 1sccm and (c) 0.5sccm, respectively.....	74
5.6	The SEM photograph of boron-doped diamond-like carbon emitters with various doping concentration (a) 2sccm, (b) 1sccm and (c) 0.5sccm, respectively.....	75
5.7	The Raman spectrum of samples A, B, C grown at different methane concentration.....	77
5.8	The Raman spectrum of samples D, E, F grown at different phosphorus concentration.....	78
5.9	The Raman spectrum of samples G, H, I grown at different boron concentration.....	79
5.10	A SIMS depth profile of phosphorus (note: only qualitative analysis).....	80
5.11	A SIMS depth profile of boron (note: only qualitative analysis).....	81
5.12	The J_e -V curve of undoped; phosphorus-doped and boron-doped diamond emitters and an insert of Fowler-Nordheim plot.....	83
6.1	SEM photographs of CNTs grown with CH_4/H_2 under (a) -120V; (b) -80V and (c) 0V, respectively.....	92
6.2	SEM photographs of CNTs grown under (a) +40V; (b) +80V and (c) +120V,	

respectively	93
6.3 Diameter of CNTs grown with CH ₄ /H ₂ as a function of applied biases	94
6.4 Schematic of the models of (a) negative and (b) positive bias effects.....	97
6.5 TEM images of CNTs grown with CH ₄ /H ₂ under (a) positive and (b) negative biases	98
6.6 (a) Raman spectra of CNTs grown with CH ₄ /H ₂ under various biases and (b) the I _D /I _G ratio as a function of applied biases	100
6.7 The I-V curve and an insert of F-N plot of CNTs grown with CH ₄ /H ₂ under (a) +120 V, (b) 0 V and (c) -120 V, respectively.....	103
6.8 SEM photographs of CNTs grown with CH ₄ /CO ₂ under (a) 0V; (b) -40V and (c) -150V, respectively	106
6.9 SEM photographs of CNTs grown with CH ₄ /CO ₂ under (a) +40V; (b) +150V and (c) 0V, respectively	107
6.10 Diameter of CNTs grown with CH ₄ /CO ₂ as a function of applied biases.....	108
6.11 TEM images of CNTs grown with CH ₄ /CO ₂ under (a) positive and (b) negative biases	109
6.12 EDX spectrum of CNTs grown with Pd catalyst	110
6.13 The I-V curve of CNTs grown with CH ₄ /H ₂ and CH ₄ /CO ₂ , respectively.....	112
6.14 (a) top view, (b) low magnification and (c) high magnification SEM photographs of carbon nanofibers grown with CH ₄ /CO ₂ under applied -100 V on catalyst-free soda-lime glass	116
6.15 SEM photographs of carbon nanofibers grown with CH ₄ /CO ₂ under various applied biases on catalyst-free soda-lime glass (a) 0 V, (b) -50 V and (c) -130, respectively	117
7.1 SEM photographs of undoped CNT film (a) cross-section view, (b) low magnification and (c) high magnification view	125
7.2 SEM photographs of undoped-CNT films grown on the backside of substrate	126
7.3 SEM photographs of coiled carbon nanotubes	128
7.4 SEM photographs of (a) undoped and (b) boron-doped CNTs arrays	129
7.5 TEM images of undoped CNTs	131
7.6 TEM images of boron-doped CNT with various boron concentration at (a) 1 sccm and (b) 2 sccm	132
7.7 Raman spectrum of undoped and various concentrations of boron-doped CNTs	

.....	135
7.8 I_D/I_G ratio of undoped and various concentrations of Boron-doped CNTs...	136
7.9 A SIMS depth profile of boron	137
7.10 Current density (J)- electric field (E) curve of undoped CNTs films, undoped and boron-doped CNTs arrays	139
7.11 F-N plot of (a) undoped and (b) boron-doped CNTs arrays	140
7.12 Electrical resistivities of carbon nanotubes film with various -boron concentration under room temperature	142
8.1 SEM photographs of carbon nanotips grown on Pt under (a)–80V and (b)–150V	150
8.2 SEM photographs of carbon nanotips grown under –120V on (a) Pt and (b) Si	151
8.3 TEM images and diffraction pattern of (a) the end section and (b) lateral section of an individual tip	153
8.4 Raman spectra of carbon nanotips grown under various biases and substrates....	154
8.5 The current density versus electric field and F-N plot of carbon nanotips grown under –120V on (a) Pt and (b) Si	157
8.6 SEM photographs of nanotips grown under (a) -100V, (b) -130V and (c) -150V ...	160
8.7 TEM images and Fourier filtering transformation (FFT) of (a) the end section and (b) lateral section of an individual tip	163
8.8 Raman spectra of nanotips growing under different applied biases	164
8.9 The emission current versus the gate voltage of nanotips on a gated device structure.....	165
9.1 SEM photographs of (a) cross-section view; (b) top view and (c) high magnification images of CNTWNCCs	175
9.2 TEM images of (a) cross-section view; (b) individual of CNTWNCCs and (c) the lateral section of carbon nanotip.....	176
9.3 (a) TEM images; and (b) diffraction pattern (DP) (c) EDX spectrum of nanocrystalline chromium carbide, respectively	177
9.4 (a) EDX and (b) EELS spectrum of nanocrystalline chromium carbide, respectively	178
9.5 (a) The current density (J) versus electric field (E) and (b) F-N plot of CNTWNCCs	181